

where  $2a$  is the impact parameter and  $v_i$  is the initial incoming velocity at  $t = -\infty$ . The quadrupole formula<sup>11</sup> leads to the result  $D = 2.466$ . The reason for this discrepancy is that we have consistently taken into account the reaction terms  $-\frac{11}{3}Gm^2[\ ]$  in formula (8) and the terms from the second-order metric  $F_2^\mu$  in formula (8) which in the near zone give a contribution as large as those from the linear terms in  $F_1^\mu$ . I therefore conclude that the quadrupole formula cannot be applied to calculate the energy loss of the source for small-angle scattering. The bound-state problem is, of course, open, but it would be remarkable if the quadrupole formula worked there but not in the small-angle-scattering case.

I would like to thank the members of the Relativity Group at the Max Planck Institute for helpful discussions. In particular I would like to thank Jürgen Ehlers, Martin Walker, Demetrios Christodoulou, and Bernd Schmidt for useful critical remarks.

<sup>1</sup>J. Ehlers, A. Rosenblum, J. Goldberg, and P. Havas, *Astrophys. J. Lett.* **208**, L77 (1976).

<sup>2</sup>*Isolated Gravitating Systems in General Relativity*, edited by J. Ehlers (North-Holland, Amsterdam, to be published).

<sup>3</sup>*Proceedings of the International School of General Relativistic Effects in Physics and Astrophysics: Experiment and Theory*, Erice, Italy, August 1977, edited by Jürgen Ehlers (to be published).

<sup>4</sup>A. Eddington, *Theory of Relativity* (Cambridge Univ. Press, Cambridge, England, 1952), p. 251.

<sup>5</sup>A. Papapetrou, *Lectures on General Relativity* (Reidel, Hingham, Mass., 1974), p. 160.

<sup>6</sup>M. Walker, *Can. J. Phys.* **55**, 855 (1977).

<sup>7</sup>D. Christodoulou, private communication.

<sup>8</sup>I am grateful to D. Christodoulou for discussions of this point.

<sup>9</sup>L. Page and N. I. Adams, *Electrodynamics* (Van Nostrand, New York, 1940).

<sup>10</sup>S. F. Smith and P. Havas, *Phys. Rev.* **138**, 495 (1965).

<sup>11</sup>L. D. Landau and E. M. Lifshitz, *The Classical Theory of Fields* (Addison-Wesley, Reading, Mass., 1961), Chap. 9.

### Inclusive $\gamma$ and $\pi^0$ Production in $e^+e^-$ Annihilation

D. L. Scharre, A. Fong, T. P. Pun, A. Barbaro-Galtieri, J. M. Dorfan, R. Ely, G. J. Feldman, J. M. Feller, B. Gobbi, G. Hanson, J. A. Jaros, B. P. Kwan, P. Lecomte,<sup>(a)</sup> A. M. Litke, D. Lücke, R. J. Madaras, J. F. Martin, D. H. Miller, S. I. Parker, M. L. Perl, I. Peruzzi,<sup>(b)</sup> M. Piccolo,<sup>(b)</sup> P. A. Rapidis, M. T. Ronan, R. R. Ross, T. G. Trippe, V. Vuillemin, and D. E. Yount

*Stanford Linear Accelerator Center and Department of Physics, Stanford University, Stanford, California 94305, and Lawrence Berkeley Laboratory and Department of Physics, University of California, Berkeley, California 94720, and Department of Physics and Astronomy, Northwestern University, Evanston, Illinois 60201, and Department of Physics and Astronomy, University of Hawaii, Honolulu, Hawaii 96822*

(Received 1 August 1978)

We have measured inclusive  $\gamma$  and  $\pi^0$  production in multiprong events produced by  $e^+e^-$  annihilation in the center-of-mass energy range 4.9 to 7.4 GeV. We find the  $\pi^0$  inclusive cross section to be consistent in shape and normalization with half the charged- $\pi$  cross section between  $x = 0.15$  and  $0.60$ , with an integrated inclusive cross-section ratio of  $\sigma(\pi^0)/[\sigma(\pi^+) + \sigma(\pi^-)] = 0.47 \pm 0.10$ .

This Letter reports for the first time inclusive  $\gamma$  and  $\pi^0$  spectra in  $e^+e^-$  annihilation at high energy. Previous analyses of charged-particle inclusive spectra at high energy in  $e^+e^-$  annihilation have indicated that only approximately 50% of the produced energy goes into charged particles.<sup>1</sup> By directly measuring inclusive  $\gamma$  and  $\pi^0$  production, it is possible to compare the energy going into  $\pi^0$  production with that going into charged pions. It is found that the  $\pi^0$  cross section is consistent with half the charged- $\pi$  cross section for  $\pi$  momenta between approximately

0.5 and 2.0 GeV/ $c$ .

The data were collected with the Stanford Linear Accelerator Center-Lawrence Berkeley Laboratory magnetic detector at SPEAR.<sup>2</sup>  $\gamma$ 's are detected using a system of lead-glass counters (referred to as the LGW) which replaces one octant of the magnet return yoke and covers a solid angle of approximately  $0.053 \times 4\pi$  sr.<sup>3,4</sup> Briefly, the LGW consists of two arrays of lead-glass blocks (a  $2 \times 26$  array of  $10 \times 90$ -cm<sup>2</sup> blocks 3.3 radiation lengths thick, and a  $14 \times 19$  array of  $15 \times 15$ -cm<sup>2</sup> blocks 10.5 radiation lengths thick)

and three planes of magnetostrictive spark chambers outside the 1-radiation-length aluminum coil.  $\gamma$ 's are identified by correlated energy deposits in the lead-glass blocks and tracks in the spark chambers which are not associated with charged particles detected in the central detector.  $\gamma$ 's which convert in the coil (as identified by tracks in the two spark-chamber planes situated between the coil and the inner plane of lead-glass blocks) are corrected for the average energy loss (approximately 50 MeV).  $\pi^0$  identification is accomplished by combining pairs of  $\gamma$ 's in the LGW. A background subtraction is made to statistically extract the  $\pi^0$  peak. The LGW was initially calibrated using Bhabha events. The  $\gamma$  calibration was checked (and found to be correct within uncertainties) by using  $\gamma$ 's from the reaction  $e^+e^- \rightarrow \gamma\gamma$  (for high-energy  $\gamma$ 's) and by checking the reconstructed  $\pi^0$  mass (for lower-energy  $\gamma$ 's). The  $\gamma$  energy resolution is  $\Delta E/E \approx 0.09/E^{1/2}$  ( $E$  in GeV), and the angular resolution is  $\Delta\theta \approx 0.5^\circ$ .

For charged particles, the analysis techniques are similar to those described previously.<sup>5</sup> The central detector consists of four layers of cylindrical spark chambers covering a solid angle of approximately  $0.60 \times 4\pi$  sr, and provides a momentum resolution of  $\Delta p/p \approx 0.013p$  ( $p$  in GeV/c). Charged-particle identification is based mainly on time-of-flight measurements over a 1.5–2.0-m flight path using a Gaussian time distribution

with a 0.35-ns standard deviation.  $\pi/K/p$  separation is clean to approximately 0.9 GeV/c in momentum.

This analysis is based on a sample of approximately 50 000 multiprong events (events with three or more prongs) in the center-of-mass energy ( $E_{c.m.}$ ) range from 4.9 to 7.4 GeV. It represents a total luminosity of  $7.5 \text{ pb}^{-1}$ . Two-prong events are eliminated from the analysis because of the large contamination from quantum-electrodynamic processes and beam-gas interactions. In the analysis, residual contamination from beam-gas interactions ( $\sim 3\%$  of the sample) is statistically subtracted based on the event vertex distribution along the beam direction.

In Fig. 1(a) is shown the inclusive  $\gamma$  cross section,  $s d\sigma/dx$ , as a function of the scaling variable  $x = 2p/E_{c.m.}$ . It is shown for three different  $E_{c.m.}$  regions, 4.9–6.0, 6.0–6.9, and 6.9–7.4 GeV, clearly showing scaling behavior. Corrections for geometric acceptance and trigger efficiency are included and are based on a two-component Monte Carlo procedure which includes hadronic events (produced with limited transverse momentum about the jet axis) and  $e^+e^- \rightarrow \tau^+\tau^-$  events.<sup>6</sup> Also included are corrections for initial-state radiation. The error bars shown reflect only the statistical errors with the exception of the lowest two points at each energy for which an additional error has been included to account

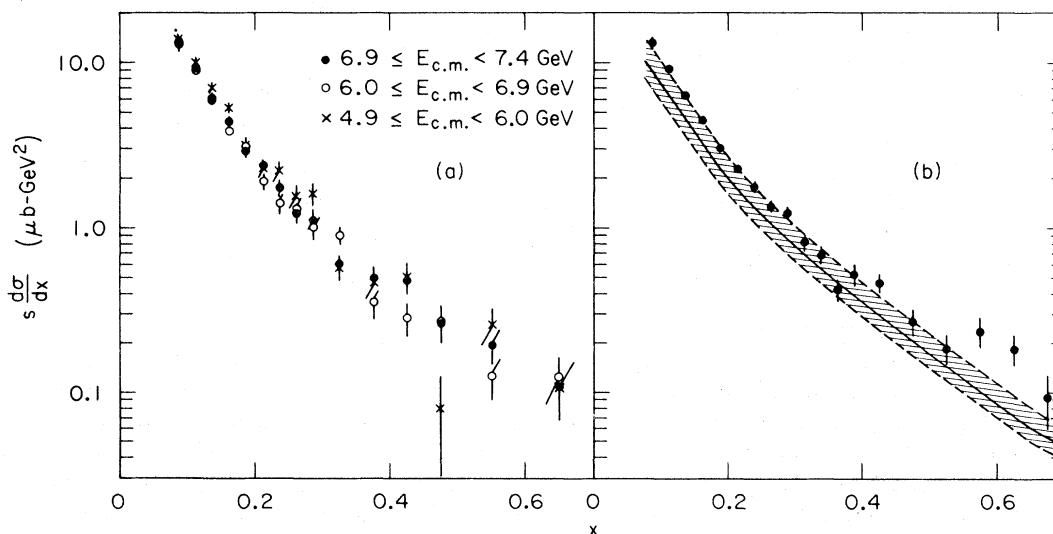


FIG. 1. (a) Inclusive  $\gamma$  cross sections,  $s d\sigma/dx$ , as functions of  $x$  for the  $E_{c.m.}$  regions 4.9–6.0, 6.0–6.9, and 6.9–7.4 GeV. (b) Inclusive  $\gamma$  cross section for the entire  $E_{c.m.}$  range. Curve represents the predicted cross section based on the assumptions that the  $\pi^0$  cross section is half the observed charged  $\pi$  cross section and  $\pi^0$ 's are the sole sources of  $\gamma$ 's. Shaded region represents the estimated systematic error in the relative normalizations.

for the increased difficulty in calculating the acceptance for low-energy  $\gamma$ 's. An overall systematic error (not included in the error bars) of approximately  $\pm 20\%$  is roughly independent of  $x$  and mostly cancels when different distributions are compared. Figure 1(b) shows the inclusive cross section for the entire  $E_{c.m.}$  region (4.9–7.4 GeV).

To examine  $\pi^0$  production, all events with two or more  $\gamma$ 's in the LGW are considered. A minimum momentum cut of 100 MeV/c is made on each  $\gamma$  to eliminate background. All invariant-mass combinations of two  $\gamma$ 's are constructed. In order to subtract the background under the  $\pi^0$  peak, the data are partitioned according to the measured  $\gamma$ -pair momentum. An estimate of the background is made by combining  $\gamma$  pairs where each  $\gamma$  is from a different event and normalizing this distribution to the data in a mass interval well above the  $\pi^0$  mass. By comparing these two samples of events, the background as a function of momentum and invariant mass is determined.

In Fig. 2 is shown the invariant-mass distribution for all  $\gamma$  pairs with total momentum greater than 600 MeV/c. The curve is the estimated background. The background is fairly small in this momentum range, but gets progressively worse at lower momenta. It is impossible to separate  $\pi^0$ 's with momenta less than approximately 400 MeV/c from the background.

Figure 3 shows the inclusive  $\pi^0$  cross section,  $s d\sigma/dx$ , as a function of  $x$ , corrected for geometric acceptance, trigger efficiency, and initial-

state radiation. In addition to the statistical error, each datum point contains a systematic error (ranging from  $\pm 20\%$  for the lowest  $x$  point to  $\pm 10\%$  for the highest  $x$  point) added in quadrature, which reflects the uncertainty in the background subtraction. The curve is half the inclusive charged- $\pi$  cross section.<sup>7</sup> The shaded region between the dashed curves represents the estimated  $\pm 20\%$  systematic error in the relative normalizations of the inclusive  $\pi^+$  and  $\pi^0$  cross sections. Within errors, the two cross sections agree over the range of measurement. If these two inclusive cross sections are integrated over the region  $x=0.15$  to  $x=0.60$ , the relative  $\pi^0$  to  $\pi^+$  production is  $\sigma(\pi^0)/[\sigma(\pi^+) + \sigma(\pi^-)] = 0.47 \pm 0.10$ , where the  $\pm 20\%$  systematic error is included in the relative normalizations.

It is of interest to determine whether the observed  $\pi^0$  production can account for the observed  $\gamma$  production. Because of the large errors and limited  $x$  range in the  $\pi^0$  production cross section, we have taken half the charged cross section shown in Fig. 3, and assumed equal  $\pi^0$  production. From this, a  $\gamma$  spectrum can be obtained which is shown as the solid curve in Fig. 1(b). Again the shaded region represents the uncertainty in the relative normalizations. The observed  $\gamma$  cross section is consistently higher than that attributed to  $\pi^0$ 's where  $\sigma(\pi^0) = \frac{1}{2}[\sigma(\pi^+) + \sigma(\pi^-)]$ . However, this excess may not be significant when account is taken of the systematic errors. If this excess is real, it could be explained by  $\eta^0$  production on the order of half the

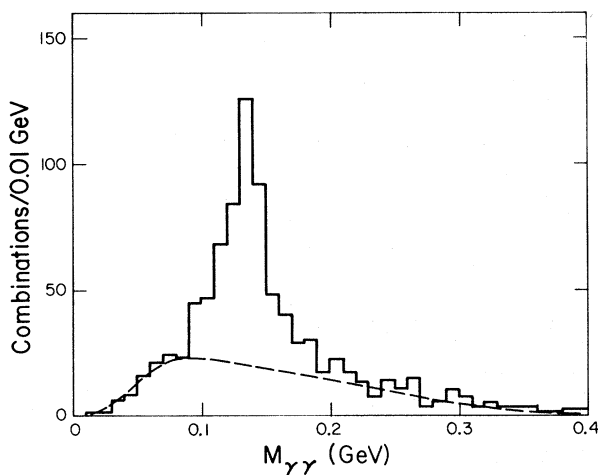


FIG. 2. Invariant-mass distribution for  $\gamma$  pairs with total momentum greater than 600 MeV/c. Background curve results from combinations taking  $\gamma$ 's from different events.

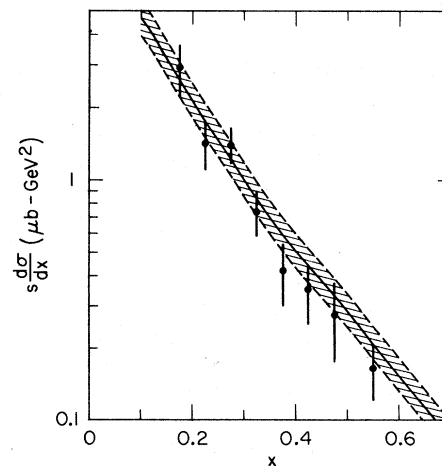


FIG. 3. Inclusive  $\pi^0$  cross section as a function of  $x$ . Curve is half the inclusive charged- $\pi$  cross section. Shaded region represents the uncertainty in the relative normalizations.

$\pi^0$  production.<sup>8</sup> Unfortunately, the small solid angle of the LGW does not permit direct observation of  $\eta^0$ 's.

In conclusion, there is no evidence that  $\pi^0$  production is significantly different from  $\pi^+$  or  $\pi^-$  production. There may be some excess production of  $\gamma$ 's over what is predicted from the measured  $\pi^0$  production cross section.

This work was supported primarily by the U. S. Department of Energy. Support for individuals came from the listed institutions plus the Deutsche Forschungsgemeinschaft, the Laboratori Nazionali di Frascati dell'Istituto Nazionale di Fisica Nucleare, and the Swiss National Science Foundation.

<sup>(a)</sup>Present address: Deutsches Elektronen-Synchrotron (DESY), Hamburg, Germany.

<sup>(b)</sup>Present address: Laboratori Nazionali di Frascati, Rome, Italy.

<sup>1</sup>R. F. Schwitters, in *Proceedings of the International Symposium on Lepton and Photon Interactions at High Energies, Stanford, California, 1975*, edited by W. T. Kirk (Stanford Linear Accelerator Center, Stanford, Calif., 1975), p. 5.

<sup>2</sup>J.-E. Augustin *et al.*, Phys. Rev. Lett. **34**, 764 (1975).

<sup>3</sup>J. M. Feller *et al.*, IEEE Trans. Nucl. Sci. **25**, 304 (1977).

<sup>4</sup>D. L. Scharre *et al.*, Phys. Rev. Lett. **40**, 74 (1978).

<sup>5</sup>G. Goldhaber *et al.*, Phys. Rev. Lett. **37**, 255 (1976).

<sup>6</sup>The relative insensitivity of the acceptance and trigger efficiency to major changes in the Monte Carlo calculation gives confidence in these corrections. The major uncertainty arises from the correction for events with zero or two produced prongs which are not in the data sample.

<sup>7</sup>This measurement is similar to previous measurements of the inclusive charged-particle spectrum [see G. G. Hanson, SLAC Report No. SLAC-PUB-2118, [in Proceedings of the Thirteenth Rencontre de Moriond on High-Energy Leptonic Interactions and High-Energy Hadronic Interactions, 1978 (to be published)]]; The major change involves elimination of tracks which are not pions.  $K$ 's and  $p$ 's are eliminated by time-of-flight separation. (At higher momentum, the separation is based on extrapolation from the lower-momentum data.) Muon and electron contamination (on the order of a few percent) is corrected for in the Monte Carlo acceptance calculation.

<sup>8</sup>One of us (D.L.S.) has addressed the question of whether all of the center-of-mass energy can be accounted for by extrapolation of the observed inclusive particle cross sections to low momentum. This extrapolation was done using a jet-model Monte Carlo which includes effects due to the rest masses of heavy particles (kaons and nucleons), missing neutral kaons, neutrinos from  $\tau$ , and charmed-particle decays, and we have made the additional, untested assumption that there is  $\eta^0$  production on the order of 50% or more of the  $\pi^0$  production. With these assumptions, this model can account for both the charged and neutral inclusive cross sections with no unaccounted-for energy.

## Cross-Section Measurements for the Reactions $\nu p \rightarrow \mu^- \pi^+ p$ and $\nu p \rightarrow \mu^- K^+ p$ at High Energies

J. Bell, J. P. Berge, D. V. Bogert, R. J. Cence, C. T. Coffin, R. N. Diamond, F. A. DiBianca, R. Endorf, H. T. French, R. Hanft, F. A. Harris, M. Jones, C. Kochowski, W. C. Louis, G. R. Lynch, J. A. Malko, J. P. Marriner, G. I. Moffatt, F. A. Nezzrick, M. W. Peters, V. Z. Peterson, B. P. Roe, R. T. Ross, W. G. Scott, A. A. Seidl, W. Smart, V. J. Stenger, M. L. Stevenson, J. C. Vander Velde, and E. Wang  
*Fermi National Accelerator Laboratory, Batavia, Illinois 60510, and Lawrence Berkeley Laboratory, Berkeley, California 94720, and University of Hawaii at Manoa, Honolulu, Hawaii 96822, and University of Michigan, Ann Arbor, Michigan 48109*

(Received 26 July 1978)

We present results for the reactions  $\nu p \rightarrow \mu^- \pi^+ p$  and  $\nu p \rightarrow \mu^- K^+ p$  at energies above 5 GeV. The average cross section for the first reaction between 15 and 40 GeV is  $(0.80 \pm 0.12) \times 10^{-38} \text{ cm}^2$  and for events with  $M_{\pi^+ p} < 1.4 \text{ GeV}$  is  $(0.55 \pm 0.08) \times 10^{-38} \text{ cm}^2$ . The ratio of the cross section for the second reaction to that for the first is  $0.017 \pm 0.010$ .

We present results for the reactions  $\nu p \rightarrow \mu^- \pi^+ p$  and  $\nu p \rightarrow \mu^- K^+ p$  obtained from a 150 000-picture exposure of the Fermilab 15-ft bubble chamber, filled with hydrogen, to a wide-band horn-focused neutrino beam. The neutrino-event energy

spectrum is roughly flat between 10 and 30 GeV then falls off such that  $\sim 90\%$  of the spectrum is below 100 GeV. Details of the scanning, measurement, and reconstruction procedures will be given elsewhere.<sup>1</sup>